

Frequency- and electric field-dependent physical model of ferroelectric materials in the tens of GHz*

Aaron M. Hagerstrom*, Eric Marksztz*[†], Christian J. Long*, James C. Booth*, Ichiro Takeuchi[†], Nathan D. Orloff*

*National Institute of Standards and Technology [†]University of Maryland

Abstract—Ferroelectric materials are attractive for tunable components because their permittivity can be controlled by an applied electric field. The permittivity of these materials also depends on frequency, and can have a strongly nonlinear electric field dependence. A quantitative understanding of these behaviors is relevant for integration of tunable materials into devices. In this paper, we provide a simple closed-form expression for this dependence, which to our knowledge has never appeared in the literature. This expression is based on thermodynamic principles, and we expect it to be both widely applicable and generalizable. We test this model with measurements of transmission lines lithographically patterned on a ferroelectric thin film, and find that the relaxation timescales become shorter at higher bias fields. We attribute this faster relaxation to the steepening of the free energy gradient when a bias field is applied.

Index Terms—tunable microwave materials, tunable components, materials characterization, functional materials, device modeling

I. INTRODUCTION

Tunable dielectric materials are an attractive solution for frequency-agile microwave components because their permittivity can be tuned by an applied electric field. This field-dependent permittivity translates into a variable capacitance, which can be used to build voltage-tunable filters, phase shifters, and other components [1], [2]. In particular, reconfigurable phase shifters are a key enabling technology for phased array antennas, which will be employed in 5G [3] communications systems operating in the tens of GHz. To design tunable devices, we need to have a quantitative understanding of the tuning behavior of any materials involved. The alternative is costly iterations of trial and error design. Simple, closed-form models are convenient when available. An accurate and simple model of ferroelectric capacitors based on thermodynamic theory was provided by [4]. However, this model does not attempt to describe frequency dependence of the material, which is an important physical feature of nonlinear dielectrics. Ferroelectric materials often have relaxation processes that are active in the tens of GHz [5], [6].

In this paper, we present a thermodynamic model for the electric field and frequency dependence of ferroelectric materials based on very general physical considerations. We test this model by measuring coplanar waveguides (CPWs) lithographically patterned on a thin film of Ba_{0.5}Sr_{0.5}TiO₃

(BST). We find good agreement between our model and our measurements.

II. MODEL

The tuning of ferroelectric materials with an electric field is often described in terms of a free energy G with an anharmonic dependence on the polarization P [4], [7]:

$$G = \frac{1}{2}\alpha P^2 + \frac{1}{4}\beta P^4 + \dots \quad (1)$$

Here, α and β are coefficients that describe the shape of the potential well. In equilibrium, the electric field is $E = \partial G / \partial P$.

A frequency-dependent model must describe how the material responds in time to an applied perturbation. In the Landau-Khalatnikov model, the material displays Debye-like relaxation with time constant τ [7]:

$$\tau \frac{dP}{dt} + P = \varepsilon_0 \varepsilon_s [E(t) - \beta P^3], \quad (2)$$

where ε_0 is the permittivity of free space and $\varepsilon_s = \varepsilon_0 / \alpha$.

Equation (2) does not accurately describe BST, because BST has a more complex time dependence. At microwave frequencies, BST shows dispersion over a wider range of frequencies. This dispersion can be described as a distribution of relaxation times, which are attributed to polar nano-regions (PNRs) [8]. According to [9], the distribution of relaxation times corresponds to a statistical distribution of sizes of PNRs. Acknowledging the non-Debye relaxation behavior of materials with PNRs, Glazounov and Tagantsev proposed a more general model which reduces to Equation (2) as a special case [7]:

$$P(t) = \varepsilon_0 \varepsilon_s \int_{-\infty}^{\infty} dt' f(t-t') [E(t) - \beta P^3(t)]. \quad (3)$$

Equation (3) accommodates very general time-domain dynamics: $f(t-t')$ could potentially describe any linear, time-invariant behavior. These dynamics may also be expressed in the frequency domain via the Fourier transform $\hat{f}(\omega) = \int dt f(t) \exp(-j\omega t)$. For BST, the distribution of relaxation times has been phenomenologically parameterized by the Cole-Cole model, which we employ in this paper [5]:

$$\hat{f}(\omega) = \frac{1}{1 + (j\omega\tau)^a} \quad (4)$$

In Equation (4), τ and a are empirical parameters. The special case $a = 1$ corresponds to Equation (2).

* This paper is an official contribution of the US government; it is not subject to copyright in the US.

To derive a frequency- and electric field-dependent model, we Taylor-expand Equation (3) to first order about a large dc bias field. To do this, we write the electric field and polarization as $E(t) = E_{dc} + e \exp(j\omega t)$ and $P(t) = P_{dc} + p \exp(j\omega t)$. This linearization of Equation (3) yields:

$$P_{dc} = \varepsilon_0 \varepsilon_s [E_{dc} - \beta P_{dc}^3], \quad (5)$$

$$p = \varepsilon_0 \varepsilon_s \hat{f}(\omega) [e - 3\beta P_{dc}^2 p]. \quad (6)$$

The numerical value of β can be hard to interpret intuitively. For this reason, we use the scaled parameter

$$E_{NL} = \sqrt{\frac{4\alpha^3}{3\beta}}. \quad (7)$$

The parameter E_{NL} has units of electric field, and can be interpreted as the electric field that must be applied to tune the dc permittivity of the material by about 62% of its zero-bias value. In terms of this scaled parameter, Equation (5) can be solved in closed form [4]:

$$P_{dc} = (\varepsilon_s \varepsilon_0) E_{NL} T\left(\frac{E_{dc}}{E_{NL}}\right), \quad (8)$$

$$\text{where } T\left(\frac{E_{dc}}{E_{NL}}\right) = \sinh\left[\frac{1}{3} \sinh^{-1}\left(3 \frac{E_{dc}}{E_{NL}}\right)\right]. \quad (9)$$

The function $T(\cdot)$ describes the tunability of the material. For small arguments, this function is approximately linear with a slope of 1, but it begins to saturate as $E_{dc} \sim E_{NL}$.

Equation (6) can be rearranged to describe the frequency- and electric field- dependent susceptibility, $\chi = p/\varepsilon_0 e$:

$$\chi(\omega, E_{dc}) = \varepsilon_\infty + \frac{\varepsilon_s \hat{f}(\omega)}{1 + 4T\left(\frac{E_{dc} - E_c}{E_{NL}}\right)^2 \hat{f}(\omega)}. \quad (10)$$

For the remainder of this paper, we choose $\hat{f}(\omega)$ to be given by Equation (4) because this function fits our data well, but this is not essential to the theory. We have also added a parameter E_c , the coercive electric field, to reflect that our sample has a small amount of hysteresis at room temperature, and ε_∞ , to model non-tunable contributions to the polarization. Thus, the parameters in our model are a , τ , ε_s , ε_∞ , E_{NL} , and E_c .

III. EXPERIMENT

To test our model, we deposited a 1 μm -thick $\text{Ba}_{0.5}\text{Sr}_{0.5}\text{TiO}_3$ film by pulsed laser deposition on a LaAlO_3 substrate. In order to measure the permittivity, we lithographically patterned gold coplanar waveguides on the sample. The metalization thickness was 500 nm, and the ground planes had a width of 200 μm , the center conductor had a width of 20 μm , and the gap widths were 5 μm .

To characterize the permittivity, we performed on-chip scattering parameter measurements. We measured 6 CPWs whose lengths varied from 0.420 mm to 7.000 mm. Our network analyzer was calibrated to the probe tips by a multiline Thru-Reflect-Line calibration on a reference substrate with a known capacitance per unit length [10]. The dc bias voltage was applied between the center conductor and the ground planes

by use of a bias tee. Electric field values are estimated from the bias voltage divided by the gap width.

We then determined the permittivity from the distributed circuit parameters of the CPWs: the inductance L , resistance R , capacitance C and conductance G . We assume that the electromagnetic fields of the waveguide mode are confined to the transverse direction (TEM propagation). This assumption is common in the literature [5], but we hope to evaluate its accuracy in the future. If the mode is TEM, R and L do not depend on the permittivity of the sample, but C and G are proportional to the real and imaginary permittivity, respectively [11]. Thus R and L can be estimated through quasi-static finite element simulations. From the scattering parameters, we can estimate the propagation constant, γ , given by $\gamma = \sqrt{(R + j\omega L)(G + j\omega C)}$ [10]. Thus we can estimate C and G for our transmission lines, which can be used to determine the permittivity. The permittivity is related to C and G in a straightforward way:

$$C + \frac{G}{j\omega} = c_0 + c_1 \varepsilon(\omega). \quad (11)$$

Equation (11), along with the values of c_0 and c_1 was derived analytically [12], but we determined the constants c_0 and c_1 from quasi-static finite element simulations.

IV. RESULTS

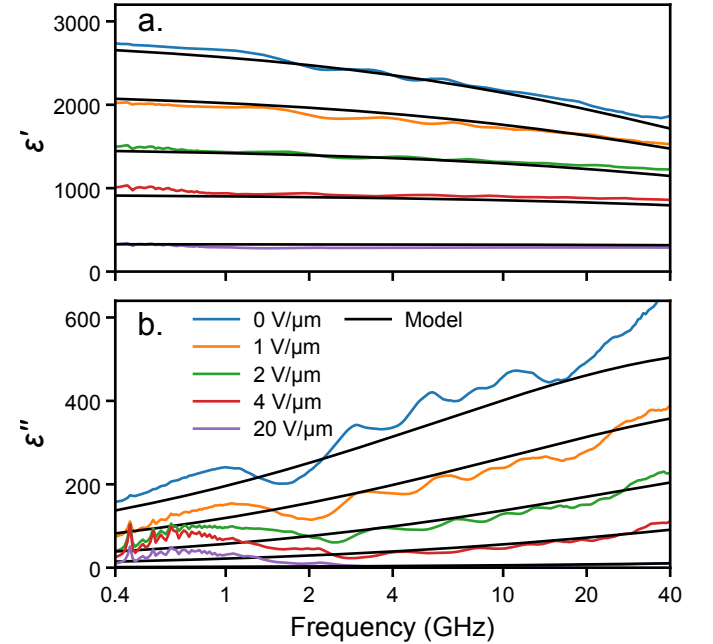


Fig. 1: Frequency dependence of the a) real and b) imaginary parts of the complex permittivity at different bias electric fields. We have used the notation $\varepsilon = 1 + \chi = \varepsilon' - j\varepsilon''$.

Fig. 1 shows the frequency dependence of the complex permittivity for several values of the bias electric field, and a fit of the model to the data. The fit parameters were: $E_{NL} = 3.04 \text{ V}/\mu\text{m}$, $E_c = -0.06 \text{ V}/\mu\text{m}$, $a = 0.46$, $\tau = 1.9$

ps, $\epsilon_s = 2760$, and $\epsilon_\infty = 70$. Anticipating that our sample may exhibit hysteresis, we swept the field from 0 up to 20 V/ μm , down to -20 V/ μm , and up again. Here, we plot the 2nd increasing sweep. We note small variations in the frequency dependence, which we attribute to imperfections in our calibration. The loss, ϵ'' , increases with frequency, and both the real and imaginary parts of the permittivity decrease with applied electric field.

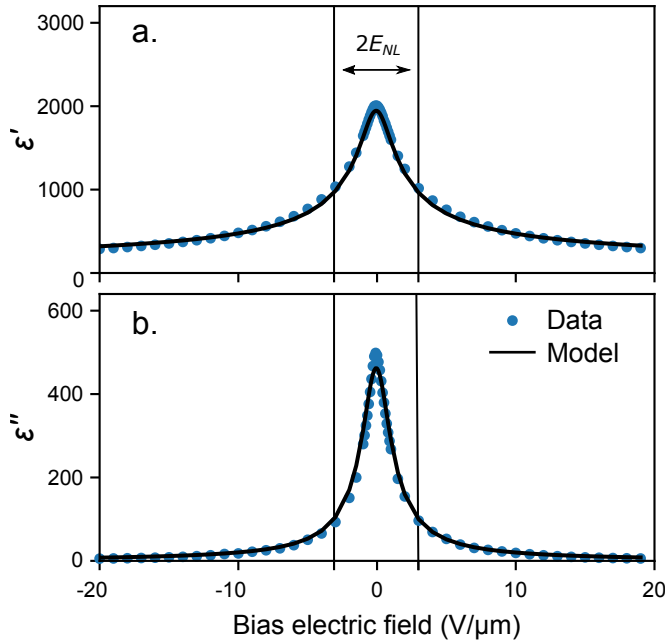


Fig. 2: Electric field dependence of the a) real part of the permittivity and b) imaginary part of the permittivity at 20 GHz. An interval of width $2E_{NL}$ centered on the peak value is indicated, showing that E_{NL} is a characteristic scale for the tunability. Note that ϵ'' tunes more strongly (82 % at E_{NL}) than ϵ' real part (49 %).

The imaginary part of the permittivity (ϵ'') tunes more strongly with bias electric field than ϵ' , as seen in Figure 2, which shows the tuning of the film with applied voltage at a frequency of 20 GHz. In our model, the function $\hat{f}(\omega)$ describes the distribution of PNR sizes, and does not depend on bias field. The change in loss is a direct consequence of the P^3 term in Equation (3). So, in our model, the loss decreases with DC bias because the gradient of the free energy with respect to P is stronger when the sample is biased, so P relaxes faster.

V. CONCLUSION

We have introduced a physical model of the real and imaginary parts of the permittivity as a function of electric field and voltage. Because generalizations of Equations (1) are widely used in the ferroelectric literature, and Equation (3) is a straightforward generalization, we expect this model to be widely applicable. At the very least, the model works

for BST in the paraelectric phase at microwave frequencies. We anticipate no difficulties with this model up to the THz regime, where phonon dispersion becomes important. The biggest approximation we have made is that the electric field in the CPW gaps is constant, which is not the case. Still, the model fits the experimental data well (root-mean-square error 140 permittivity units). In addition to the variations in the data that we attribute to imperfections in the calibration, there is some voltage-dependent deviation of the model from the data that we attribute electric field inhomogeneity.

In addition to fitting a complicated data set with a few parameters, our model offers some physical insight. In particular, the imaginary part of the permittivity tunes more strongly than the real part. We interpret this in terms of the gradient of the free energy with respect to P . Finally, we note that Equation (3) also predicts higher order nonlinear dynamical behavior, including frequency dependence for intermodulation products and harmonics. This characterization is underway [13].

REFERENCES

- [1] A. K. Tagantsev, V. O. Sherman, K. F. Astafiev, J. Venkatesh, and N. Setter, "Ferroelectric materials for microwave tunable applications," vol. 11, no. 1, 2003.
- [2] E. G. Erker, A. S. Nagra, Y. Liu, P. Periaswamy, T. R. Taylor, J. Speck, and R. A. York, "Monolithic ka-band phase shifter using voltage tunable BaSrTiO₃ parallel plate capacitors," *IEEE Microwave and Guided Wave Letters*, vol. 10, no. 1, pp. 10–12, 2000.
- [3] M. Sazegar, Y. Zheng, C. Kohler, H. Maune, M. Nikfalazar, J. R. Binder, and R. Jakoby, "Beam steering transmitarray using tunable frequency selective surface with integrated ferroelectric varactors," *IEEE Transactions on Antennas and Propagation*, vol. 60, no. 12, pp. 5690–5699, 2012.
- [4] D. R. Chase, L.-Y. Chen, and R. A. York, "Modeling the capacitive nonlinearity in thin-film bst varactors," *IEEE transactions on microwave theory and techniques*, vol. 53, no. 10, pp. 3215–3220, 2005.
- [5] J. C. Booth, I. Takeuchi, and K.-S. Chang, "Microwave-frequency loss and dispersion in ferroelectric Ba_{0.3}Sr_{0.7}TiO₃ thin films," *Applied Physics Letters*, vol. 87, no. 8, p. 082908, 2005.
- [6] C.-H. Lee, N. D. Orloff, T. Birol, Y. Zhu, V. Goian, E. Rocas, R. Haislmaier, E. Vlahos, J. A. Mundy, L. F. Kourkoutis, Y. Nie, M. D. Biegalski, J. Zhang, M. Bernhagen, N. A. Benedek, Y. Kim, J. D. Brock, R. Uecker, X. X. Xi, V. Gopalan, D. Nuzhnyy, S. Kamba, D. A. Muller, I. Takeuchi, J. C. Booth, C. J. Fennie, and D. G. Schlom, "Exploiting dimensionality and defect mitigation to create tunable microwave dielectrics," *Nature: London*, vol. 502, no. 7472, pp. 532–6.
- [7] A. E. Glazounov and A. K. Tagantsev, "Phenomenological model of dynamic nonlinear response of relaxor ferroelectrics," *Physical Review Letters*, vol. 85, no. 10, pp. 2192–2195, 2000.
- [8] T. Teranishi, T. Hoshina, H. Takeda, and T. Tsurumi, "Polarization behavior in diffuse phase transition of Ba_xSr_{1-x}TiO₃ ceramics," *Journal of Applied Physics*, vol. 105, no. 5, p. 054111, 2009.
- [9] Z. Lu and G. Calvarin, "Frequency dependence of the complex dielectric permittivity of ferroelectric relaxors," *Physical Review B*, vol. 51, no. 5, p. 2694, 1995.
- [10] R. B. Marks, "A multiline method of network analyzer calibration," *IEEE Transactions on Microwave Theory and Techniques*, vol. 39, no. 7, pp. 1205–1215, 1991.
- [11] R. B. Marks and D. F. Williams, "A general waveguide circuit theory," vol. 97, no. 5, pp. 533–562, 1992.
- [12] E. Carlsson and S. Gevorgian, "Conformal mapping of the field and charge distributions in multilayered substrate CPWs," vol. 47, no. 8, pp. 1544–1552, 1999.
- [13] A. M. Hagerstrom, E. Marks, C. J. Long, J. C. Booth, and N. D. Orloff, "Characterization of transmission lines with nonlinear dielectric materials," in *90th ARFTG Microwave Measurement Symposium*. IEEE, 2017, pp. 1–6.